PNAS RESEARCH ARTICLE | NEUROSCIENCE OPEN ACCESS

Deficiency of orexin signaling during sleep is involved in abnormal REM sleep architecture in narcolepsy

Hiroto Ito[a,b,c], Noriaki Fukatsu[a,b], Sheikh Mizanur Rahaman[a,b], Yasutaka Mukai[a,b], Shuntaro Izawa[a,b], Daisuke Ono[a,b], Thomas S. Kilduff[d], and Akihiro Yamanaka[a,b,e,f,g,h,1]

Edited by Joseph Takahashi, The University of Texas Southwestern Medical Center, Dallas, TX; received February 3, 2023; accepted July 10, 2023

Narcolepsy is a sleep disorder caused by deficiency of orexin signaling. However, the neural mechanisms by which deficient orexin signaling causes the abnormal rapid eye movement (REM) sleep characteristics of narcolepsy, such as cataplexy and frequent transitions to REM states, are not fully understood. Here, we determined the activity dynamics of orexin neurons during sleep that suppress the abnormal REM sleep architecture of narcolepsy. Orexin neurons were highly active during wakefulness, showed intermittent synchronous activity during non-REM (NREM) sleep, were quiescent prior to the transition from NREM to REM sleep, and a small subpopulation of these cells was active during REM sleep. Orexin neurons that lacked orexin peptides were less active during REM sleep and were mostly silent during cataplexy. Optogenetic inhibition of orexin neurons established that the activity dynamics of these cells during NREM sleep regulate NREM–REM sleep transitions. Inhibition of orexin neurons during REM sleep increased subsequent REM sleep in "orexin intact" mice and subsequent cataplexy in mice lacking orexin peptides, indicating that the activity of a subpopulation of orexin neurons during the preceding REM sleep suppresses subsequent REM sleep and cataplexy. Thus, these results identify how deficient orexin signaling during sleep results in the abnormal REM sleep architecture characteristic of narcolepsy.

hypothalamus | orexin | calcium imaging | cataplexy | sleep

Impairment of adequate sleep duration or quality is well known to increase sleepiness and to negatively impact the quality of wakefulness. Similar homeostatic regulation occurs for rapid eye movement (REM) sleep, a state characterized by muscle atonia and desynchronized cortical activity in which theta waves are dominant in the electroencephalogram (EEG). For example, selective deprivation of REM sleep is well known to cause subsequent REM sleep rebound (1–5). Since the discovery of REM sleep in humans (6), various neural populations and mechanisms in the hypothalamus, midbrain, and basolateral amygdala have been shown to regulate the initiation, maintenance, or inhibition of REM sleep (3, 7–12). However, the precise neural mechanisms that regulate appropriate sleep architecture, particularly REM sleep, based on preceding vigilance states remain mostly unknown (8).

Narcolepsy is a sleep disorder thought to be caused by selective loss of neurons in the perifornical and lateral hypothalamic area (LHA) that produce the neuropeptides orexin A and B (also known as hypocretin-1 and -2) (13–16). The loss of orexin peptides due to orexin neuron degeneration plays a critical role in the etiology of narcolepsy (17–19). The pathophysiology of narcolepsy has two main features: difficulty in maintenance of wakefulness, manifested as excessive daytime sleepiness (20–24), and abnormal REM sleep architecture (21, 24), exemplified by frequent transitions to REM sleep and by intrusion of REM atonia into wakefulness (cataplexy and sleep paralysis). The most dramatic symptom of narcolepsy is cataplexy, the sudden loss of muscle tone during wakefulness (20–24). Abnormal REM sleep architecture in narcolepsy might be explained by an accelerated buildup of REM sleep pressure (25) and/or a lower threshold to enter REM sleep (4). Interestingly, in mice lacking the orexin peptides, REM sleep deprivation increased subsequent cataplexy (4).

The neural pathways involved in the etiology of narcolepsy have yet to be fully elucidated. Although it has been frequently proposed that orexin neurons should receive excitatory input and be activated to prevent the triggering of cataplexy (20–24), the activity of orexin neurons during cataplexy defined by EEG and electromyographic (EMG) recordings has not been directly measured in mouse models of narcolepsy in which the orexin peptides are absent. Previous reports have proposed that the loss of orexin signaling in wakefulness-promoting nuclei causes the sleepiness and sleep fragmentation characteristic of narcolepsy (20–24). Recent studies reported that orexin signaling during REM sleep also functions in the stabilization of REM sleep and induces REM sleep–like muscle atonia

Significance

Narcolepsy is a sleep disorder caused by deficient orexin signaling due to orexin neuron degeneration. However, the neural mechanisms underlying the rapid eye movement (REM) sleep-related symptomatology of narcolepsy remain unclear. We determined previously uncertain details of orexin neuron activity dynamics during NREM sleep, REM sleep, and cataplexy at the population-level by fiber photometry and at the single-neuron level by microendoscopy. Using optogenetic approaches, we found that orexin neuron activity during NREM sleep regulates NREM–REM sleep transitions whereas orexin neuron activity during REM sleep regulates REM sleep structure and cataplexy. Collectively, this study advances understanding of how orexin neurons normally regulate REM sleep architecture, and how loss of this regulation contributes to the REM sleep–related symptomatology of narcolepsy.

Author contributions: H.I. and A.Y. designed research; H.I. and S.M.R. performed experiments; S.I. and D.O. set up state-dependent photoillumination system and the fiber photometry system, respectively; H.I., N.F., S.M.R., Y.M., T.S.K., and A.Y. contributed to the data analysis and review; and H.I., T.S.K., and A.Y. wrote the paper.

The authors declare no competing interest.

This article is a PNAS Direct Submission.

[1]To whom correspondence may be addressed. Email: yamank@cibr.ac.cn.

This article contains supporting information online at https://www.pnas.org/lookup/suppl/doi:10.1073/pnas.2301951120/-/DCSupplemental.

Published October 5, 2023.

(3, 26). However, the neural mechanisms through which the loss of orexin signaling causes abnormal REM sleep architecture in narcolepsy have not been defined. Here, we determined the activity dynamics of orexin neurons during sleep and their involvement in the abnormal REM sleep architecture characteristic of narcolepsy.

Results

Activity Dynamics of Orexin Neurons during Sleep. It has been reported that in rats, 2 to 9% of orexin neurons were cFos active after NREM and REM sleep or REM sleep rebound (27, 28). Particularly, 28% of orexin neurons that sent terminals to the sublaterodorsal tegmental nucleus (SLD) were cFos active after REM sleep rebound (3). Although these studies suggest the existence of REM-active orexin neurons, more precise methods to detect the activity in vivo are warranted. Previous studies using extracellular recordings described that orexin neuron activity was the highest during wakefulness, but intermediate, low, or virtually silent in NREM and REM sleep (29–32). Although fiber photometry recordings of orexin neurons described intermittent low activity in the cell bodies during NREM sleep (33), orexin signaling occurs in the SLD projection area during REM sleep (3). These inconsistent findings may be due to the limited number of orexin neurons recorded, a limited recording period, and/or a limited resolution of activity imaging. Thus, the activity dynamics of orexin neurons during sleep warrant a more comprehensive study at both the single-cell and population levels, and across many sleep/wakefulness state changes by extensive observations for prolonged periods.

To reveal activity dynamics of the orexin neurons across physiological sleep/wakefulness states in detail, we conducted fiber photometry recordings with EEG and EMG in freely moving mice for 24 h. To express the Ca^{2+} indicator GCaMP6s specifically in orexin neurons, AAV9-TetO-GCaMP6s was injected into the LHA of *orexin-tTA* mice (Fig. 1*A*). Immunohistochemical analysis (n = 3) confirmed that, of the neurons labeled for GCaMP6s, 93.8 ± 1.2% of them also expressed orexin-A (ratio of orexin neurons/GCaMP6s-expressing neurons) and, of the neurons labeled for orexin-A, 91.1 ± 1.2% of them also expressed GCaMP6s (ratio of GCaMP6-expressing/orexin neurons). Only 0.7 ± 0.7% of MCH neurons expressed GCaMP6s, and 1.1 ± 1.1% of GCaMP6s positive neurons were MCH-immunoreactive (n = 3). We had previously established the relationship between GCaMP signals and firing frequency in *orexin-tTA* mice (34). For fiber photometry recordings, an optic fiber was inserted into the LHA. To quantify the activity levels between states from the recordings of six mice, we extracted every 10-min episode, which includes all three vigilance states (146 episodes, each stage (wakefulness, NREM, and REM sleep) > 1 min; Fig. 1*B*) and all transitions from NREM to REM sleep (171 transitions, each stage > 1 min; Fig. 1*B*). Consistent with previous reports (29–31), we found that orexin neurons were highly active during wakefulness compared to NREM and REM sleep (Fig. 1 *C* and *D* and *SI Appendix*, Fig. S1 *A*, *E*, and *F*). However, orexin neurons also exhibited intermittent activity during NREM sleep and continuous low-level activity (relative to Wakefulness) during REM sleep (Fig. 1 *C*–*F*). During NREM sleep, the activity of orexin neurons was correlated with a decrease in spectral power in the theta and alpha EEG bandwidths (*SI Appendix*, Fig. S1 *A*–*D*). Elevated activity of orexin neurons also occurred during microarousals (*SI Appendix*, Fig. S1 *G* and *H*). Analysis of all 171 transitions recorded from NREM to REM sleep revealed a reduction of activity prior to almost every transition to REM sleep (166 out of 171; Fig. 1*E* and *SI Appendix*, Fig. S2*A*). Specifically, the mean activity of orexin neurons in each mouse was significantly reduced in the 30 sec prior to the transition from NREM to REM sleep (tNR: defined as the last 30 sec just prior to REM sleep, See also *Materials and Methods*) compared to NREM sleep and subsequent REM sleep (Fig. 1*F*). These results suggest that orexin neurons become quiescent prior to the transition to REM sleep.

For direct observation of the activity dynamics of orexin neurons at single-cell resolution, we undertook microendoscopy recordings using nVista (Fig. 2 *A* and *B*). Of the 137 cells recorded from five mice, approximately half of the orexin neurons (47.4%, 65 cells) were essentially quiescent but showed occasional intermittent activity during NREM sleep, and a smaller subpopulation was also active during REM sleep (Fig. 2 *C*–*F* and Movie S1). Of the recorded cells, almost one-third (32.1%, 44 cells) were classified as belonging to the subpopulation active during REM sleep (Fig. 2 *E* and *F*). To further evaluate the intermittent activity of orexin neurons during NREM sleep, we conducted cluster analysis by nonnegative matrix factorization (NMF) (35) in the five mice. The synchronous activity (intensity in Fig. 2*G*; representative sample) in each NREM cluster (*Materials and Methods*) and its contribution to each NREM cluster (Fig. 2*D*) was calculated using NMF. To quantify the change in the neural network, we computed pairwise correlation coefficients for all pairs of NREM-active cluster cells (*Materials and Methods*) across vigilance states. We found the largest proportion of correlated (>0.2) pairs during NREM sleep compared to other states (Fig. 2 *H* and *I*).

To evaluate whether the activity patterns of orexin neurons described above were specific to *orexin-tTA* mice, we determined the activity of orexin neurons during sleep in a different mouse strain, heterozygous *orexin-Flp (KI/-)* mice (36), which, like *orexin-tTA* mice, have orexin neurons that express orexin peptides. Synchronous cluster activity during NREM sleep and subpopulations active during REM sleep were also observed in *orexin-Flp (KI/-)* mice (*SI Appendix*, Fig. S3 and Movie S2). Thus, identical results in two strains of genetically engineered (knockin and transgenic) mice indicate that it is very unlikely that the observed phenomena could be due to transgene introduction. Thus, the occurrence of orexin neuron activity during sleep suggests a possible role for these cells in the regulation of vigilance states.

Loss of Orexin Peptides Disrupts the Activity Dynamics of Orexin Neurons during Sleep. Since the orexin neuropeptides have a critical role in the etiology of narcolepsy (17, 19, 36, 37), we hypothesized that these peptides play an important role in orexin neuron activity during sleep in addition to their well-recognized role in maintenance of wakefulness. To address this hypothesis, we used *orexin-Flp* mice that were generated by knocking in the *Flp* transgene in-frame at the start codon of the *prepro-orexin* gene. Consequently, homozygous *orexin-Flp (KI/KI)* mice are unable to synthesize orexin peptides and thus serve as a model of narcolepsy, while heterozygous *orexin-Flp (KI/-)* mice express the orexin peptides (36). We, therefore, examined changes in activity dynamics of orexin neurons lacking orexin peptides during sleep in narcoleptic *orexin-Flp (KI/KI)* mice.

Orexin-Flp (KI/KI) mice injected with AAV9-CMV-dFRT-GCaMP6s were subjected to fiber photometry (five mice; Fig. 3*A*) and microendoscopy (five mice; Fig. 4*A*). The specificity of expression of GCaMP6s to orexin neurons was confirmed in heterozygous *orexin-Flp (KI/-)* mice (*SI Appendix*, Fig. S3*C*). Only 0.2 ± 0.1% of MCH neurons expressed GCaMP6s, and 0.6 ± 0.3% of GCaMP6s positive neurons were MCH-immunoreactive (n = 3). A relationship between the GCaMP6s signal and firing frequency was

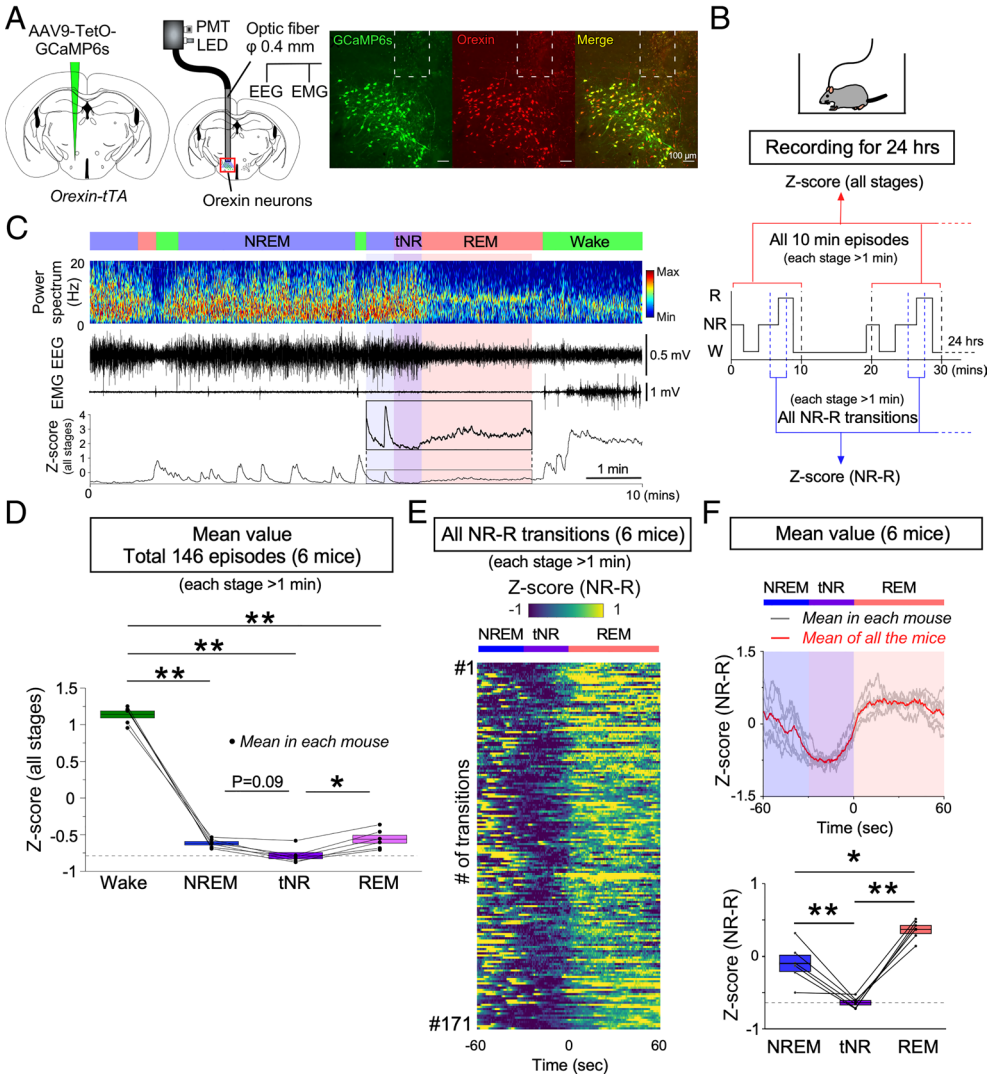

Fig. 1. Activity recordings of orexin neurons across vigilance states in *orexin-tTA* mice as determined by fiber photometry. (*A*) Schematics illustrating the injection of AAV-TetO-GCaMP6s into the LH of *orexin-tTA* mice to induce expression of GCaMP6s in orexin neurons (*Left*) and combined fiber photometry with EEG/EMG recordings (*Middle*). Immunohistochemical confirmation of GCaMP6s expression in orexin neurons (*Right*). The dashed white lines at the top of each panel indicate the edge of the optic fiber. (*B*) Schematic of experimental procedures and data analysis. (*C*) Representative orexin neuronal activity across vigilance states measured by fiber photometry. (*D*) Summary of orexin neuron activity across vigilance states, expressed as Z-scores (all stages from N = 6 mice). (*E*) Orexin neuron activity for all 171 NREM to REM transitions (each stage > 1 min) determined from 24-h recordings in N = 6 mice. (*F*, *Top*) Mean Z-score of all NREM to REM transitions for each individual mouse (gray); mean Z-score of all the N = 6 mice (red). (*F*, *Bottom*) Summary of orexin neuron activity during NREM–REM state transitions for all six mice shown as Z-scores. Values are the mean ± SEM. *$P < 0.05$, **$P < 0.01$. Statistical analyses are shown in *SI Appendix*, Table S1. Vigilance state parameters of *orexin-tTA* mice (n = 6) in the fiber photometry experiments (24 h) and the 10-min episodes for Z-score (all stages) are described in *SI Appendix*, Tables S2 and S3, respectively. tNR, last 30 s during the transition from NREM to REM sleep; PMT, photomultiplier tube; W, wakefulness; NR, NREM; R, REM.

confirmed by simultaneous patch-clamp recordings and calcium imaging in brain slices. Orexin neurons increased fluorescence intensity in an induced-action potential frequency-dependent manner (*SI Appendix*, Fig. S4).

As in nonnarcoleptic *orexin-tTA* mice, orexin neurons in narcoleptic *orexin-Flp (KI/KI)* mice that lacked orexin peptides exhibited higher activity during wakefulness and intermittent activity during NREM sleep that was closely correlated with the decreased power of the theta and alpha EEG bandwidths (Fig. 3 *B–D* and *SI Appendix*, Fig. S5 *A–F*). Also, as in *orexin-tTA* mice (*SI Appendix*, Fig. S1 *G* and *H*), orexin neuron activity was correlated with microarousals in *orexin-Flp (KI/KI)* mice (*SI Appendix*, Fig. S5 *G* and *H*). However, in contrast to *orexin-tTA* mice, orexin neuron activity in *orexin-Flp (KI/KI)* mice was lower during REM sleep than during NREM sleep or the tNR (Fig. 3 *C*, *E*, and *F*). Analysis of every transition from NREM to REM sleep (121 in total, each stage > 1 min) revealed that orexin neurons in *orexin-Flp (KI/KI)* mice showed the lowest activity during REM sleep in most of the transitions (103 out of 121; *SI Appendix*, Fig. S2*B*). However, the highest orexin neuron activity during the tNR occurred in 29 transitions (*SI Appendix*, Fig. S2*B*). These results suggest that the activity during REM sleep and the quiescence prior to the transition to REM sleep evident in *orexin-tTA* mice are impaired in narcoleptic *orexin-Flp (KI/KI)* mice in which the orexin neurons lack the orexin peptides.

As in *orexin-tTA* and *orexin-Flp (KI/-)* mice, single-cell microendoscopic imaging using nVista in five *orexin-Flp (KI/KI)* mice (Fig. 4 *A* and *B*) consistently revealed synchronous activity among orexin neurons during NREM sleep (Fig. 4 *C–E* and *G–I* and Movie S3). The largest proportion of correlated orexin neuron pairs in NREM-active cluster cells was observed during NREM sleep compared to other states (Fig. 4 *H* and *I*). However, the subpopulation of orexin neurons that were active during REM sleep (Fig. 4 *C–F*) was significantly smaller (10.1%, 7 cells) than

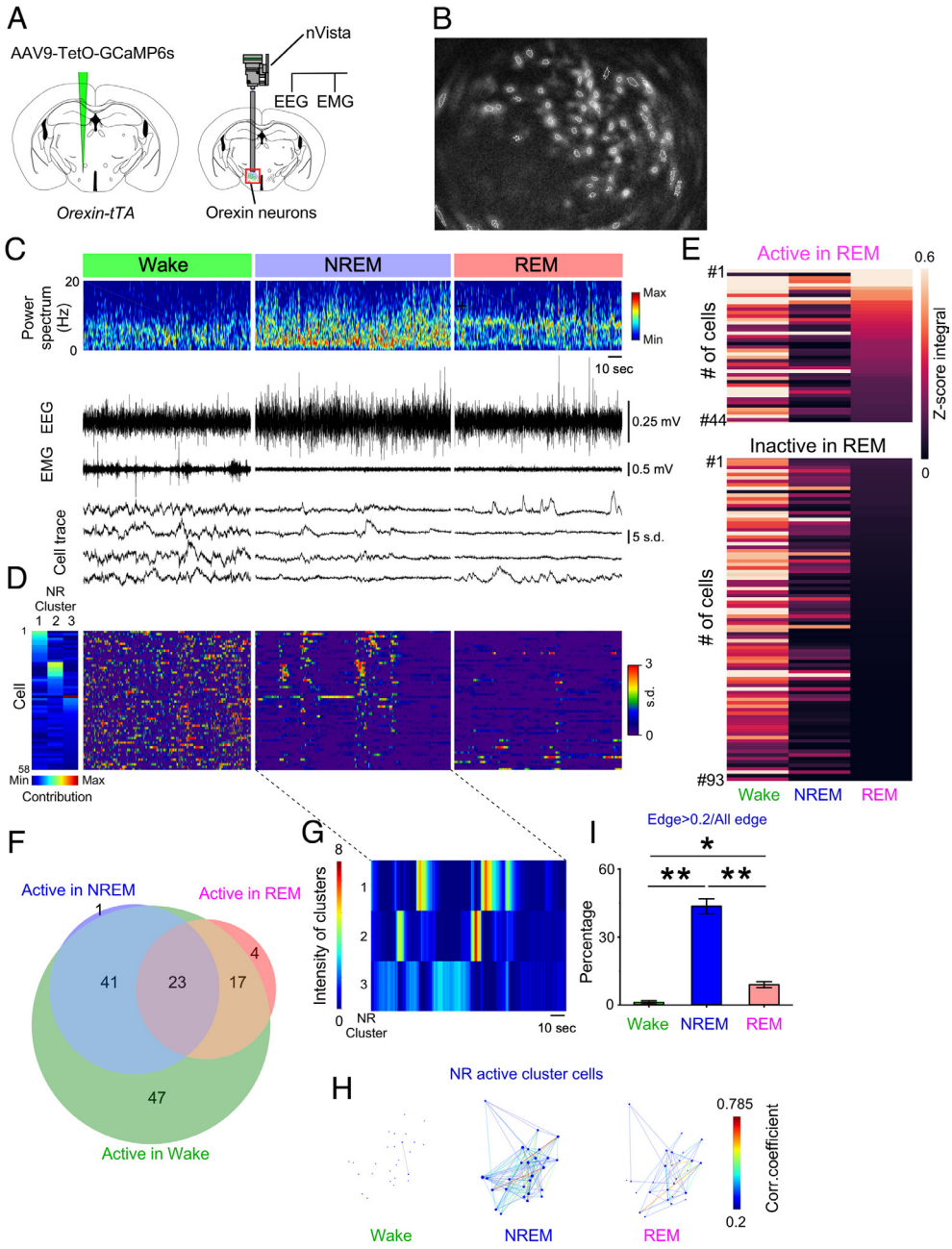

Fig. 2. Activity recordings of orexin neurons across vigilance states in *orexin-tTA* mice as determined by microendoscopy. (*A*) Schematics of GCaMP6s expression (*Left*) and nVista microendoscopy with EEG and EMG recordings (*Right*). (*B*) Representative identification of orexin neurons using nVista. Dashed white line indicates region of interest (ROI). (*C*) Representative traces of Ca^{2+} activity during each vigilance state. (*D*) Activity of orexin neurons aligned by contribution to the three NREM clusters in *G*. (*E*) Activity during each vigilance state of orexin neurons determined to be active (n = 44 cells) or inactive (n = 93 cells) during REM sleep in N = 5 mice. (*F*) Venn diagram showing the number of orexin neurons (133 cells) exhibiting each activity pattern. A total of 137 cells were detected; four neurons were not classified. (*G*) Representation of the activity of orexin neurons within NREM clusters 1, 2, and 3. (*H*) Representative correlations of activity among orexin neuron pairs from NREM-active clusters 1 and 2 in *G*. Each dot reflects the location of the cells determined by the (x, y) position of the center of the neuron in the field of view. (*I*) Percentage of cells exhibiting activity synchronization, defined by the proportion of correlated (>0.2) pairs during each vigilance state. Values are the mean ± SEM. *P < 0.05, **P < 0.01. Statistical analyses are shown in *SI Appendix*, Table S1. W, wakefulness; NR, NREM; R, REM.

in *orexin-tTA* mice (Chi-squared test, P = 0.00056) and heterozygous *orexin-Flp (KI/-)* mice (Chi-squared test, P = 0.00025; cf., Fig. 2 *E* and *F* and *SI Appendix*, Fig. S3 *F* and *G*), which express orexin peptides. The reduced activity of orexin neurons during REM sleep in the absence of orexin peptides suggests that the orexin peptides normally contribute to orexin neuron activity during REM sleep and, furthermore, that this activity may suppress the symptoms of narcolepsy such as cataplexy. Thus, these results are consistent with the hypothesis that the reduction of orexin signaling during REM sleep evident in *orexin-Flp (KI/KI)* mice is an important contributor to the symptomatology of narcolepsy.

Orexin Neurons Lacking Orexin Peptides Are Mostly Silent during Cataplexy. Several neural circuitry models of narcolepsy have proposed that orexin neurons receive excitatory inputs and should be activated to prevent the triggering of cataplexy (20–24, 38). The activity of orexin neurons during "cataplexy-like attacks" has been described by video recording (39). However, based on the consensus of the International Working Group on

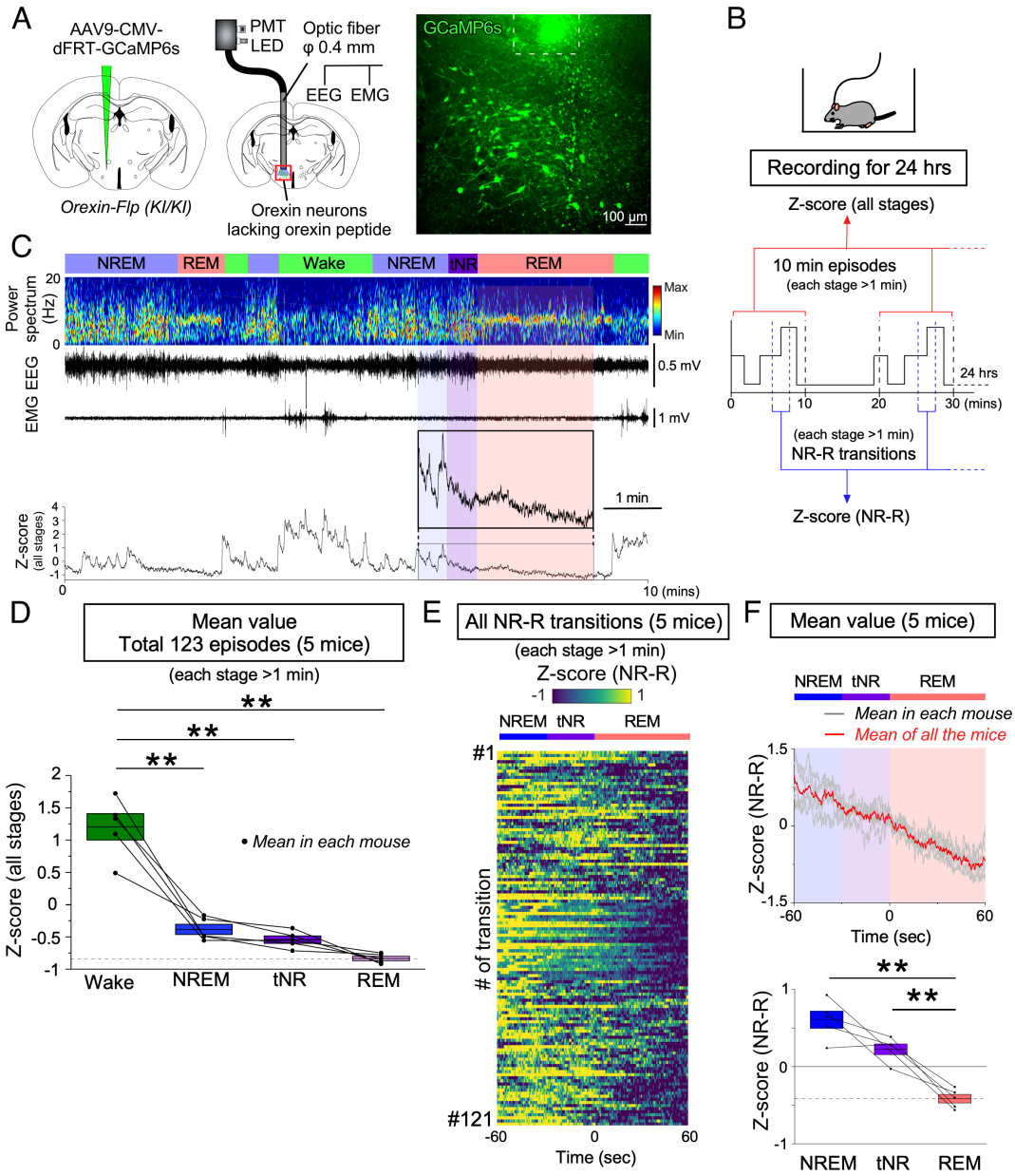

Fig. 3. Activity recordings of orexin neurons across vigilance states in prepro-orexin knockout [*orexin-Flp (KI/KI)*] mice as determined by fiber photometry. (*A*) Schematics illustrating the injection of AAV-CMV-dFRT-GCaMP6s into homozygous *orexin-Flp (KI/KI)* mice to induce expression of GCaMP6s expression in orexin neurons (*Left*) and fiber photometry with EEG/EMG recordings (*Middle*). Histochemical confirmation of GCaMP6 expression in orexin neurons (*Right*). The dashed line at the top of the panel indicates the edge of the optic fiber. (*B*) Schematic of the experimental procedures and data analysis. (*C*) Representative orexin neural activity across vigilance states measured by fiber photometry. (*D*) Summary of orexin neuron activity across vigilance states, expressed as Z-scores (all stages from N = 5 mice). (*E*) Activity of orexin neurons from all 121 NREM to REM transitions recorded (each stage > 1 min) during 24-h recordings in N = 5 mice. (*F*, *Top*) Mean Z-score of all the transitions in each individual mouse (gray); mean Z-score of all the N = 5 mice (red). (*F*, *Bottom*) Summary of orexin neuron activity of all the mice during NREM–REM state transitions shown as Z-scores. Values are the mean ± SEM. $^{*}P < 0.05$, $^{**}P < 0.01$. Statistical analyses are shown in *SI Appendix*, Table S1. Vigilance state parameters of *orexin-Flp (KI/KI)* mice (n = 5) in the fiber photometry experiments (24 h) and the 10-min episodes for Z-score (all stages) are described in *SI Appendix*, Tables S2 and S3, respectively. tNR, the last 30 s during the transition from NREM to REM sleep; PMT, photomultiplier tube; W, wakefulness; NR, NREM; R, REM.

Rodent Models of Narcolepsy (40), EEG and EMG recordings in addition to video are necessary to define cataplexy; otherwise, the term "abrupt behavioral arrest" is more appropriate when only video is used. Thus, the activity of orexin neurons during cataplexy as measured with EEG and EMG has not previously been determined in any mouse model of narcolepsy. To address this knowledge gap, we utilized *orexin-Flp (KI/KI)* mice (36) combined with fiber photometry (n = 5) and microendoscopy (n = 3) and found that most orexin neurons in *orexin-Flp (KI/KI)* mice were silent during cataplexy but quickly recovered their activity upon termination of atonia and resumption of the waking EEG (Fig. 5 *A–E*, *SI Appendix*, Fig. S6 *A–D* and Movie S4). Interestingly, although the number of the recorded neurons may be small, further analysis through recording both REM sleep and cataplexy in the same mice revealed that the subpopulation of orexin neurons that is active during REM sleep and cataplexy are almost the same [88.9% (eight out of nine neurons) for each state, *SI Appendix*, Fig. S6 *A–D*]. These results suggest either increased inhibition, a lack of excitatory inputs or both during cataplexy. Given the high frequency of spontaneous firing of orexin neurons (36, 41), inhibitory input is likely necessary to suppress spontaneous firing of orexin neurons during cataplexy.

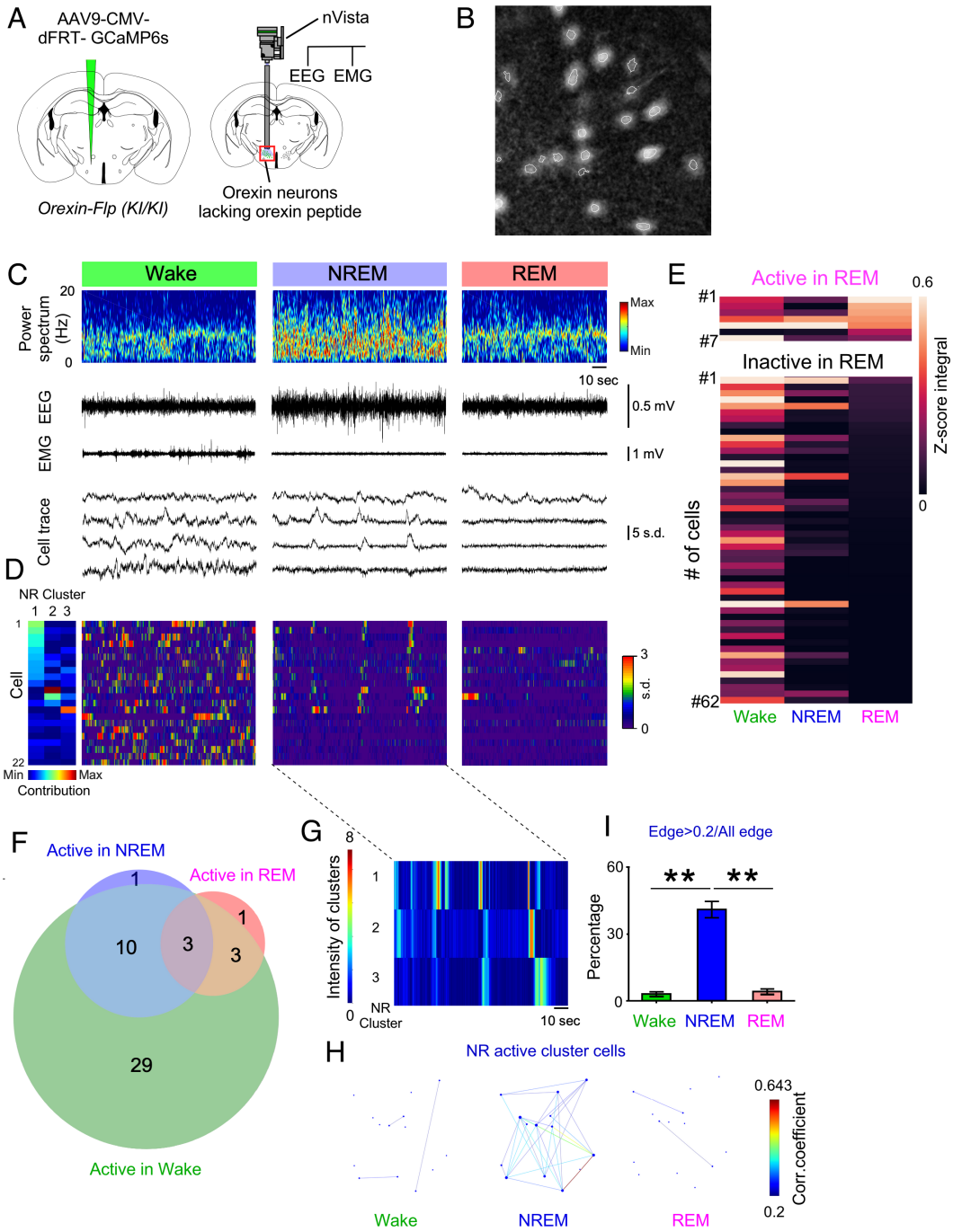

Fig. 4. Activity recordings of orexin neurons across vigilance states in prepro-orexin knockout [*orexin-Flp (KI/KI)*] as determined by microendoscopy. (*A*) Schematics of GCaMP6s expression (*Left*) and nVista microendoscopy with EEG and EMG recordings (*Right*). (*B*) Representative identification of orexin neurons using nVista. Dashed white line indicates region of interest (ROI). (*C*) Representative traces of Ca^{2+} activity during each vigilance state. (*D*) Activity of orexin neurons during NREM sleep aligned by activity cluster. (*E*) Activity during each vigilance state of orexin neurons determined to be active (7 cells) or inactive (62 cells) in REM sleep in N = 5 mice. (*F*) Venn diagram showing the number of orexin neurons (47 cells) exhibiting each activity pattern. A total of 69 cells were detected; 22 neurons were not classified. (*G*) Representation of orexin neuron activity within NREM clusters 1, 2, and 3. (*H*) Representative correlations of activity among orexin neuronal pairs in the NREM-active clusters 1 and 2 in *G*. Each dot reflects the location of the cells determined by the (x, y) position of the center of the neuron within the field of view. (*I*) Percentage of cells exhibiting activity synchronization, defined as the proportion of correlated (>0.2) pairs, during each vigilance state. Values are the mean ± SEM. $^*P < 0.05$, $^{**}P < 0.01$. Statistical analyses are shown in *SI Appendix*, Table S1. tNR, the last 30 s during the transition from NREM to REM sleep; W, wakefulness; NR, NREM; R, REM.

Optogenetic Silencing of Orexin Neurons Increases NREM–REM Sleep Transitions. Frequent transitions into REM sleep are characteristic of both the clinical presentation of narcolepsy and animal models of this disorder (19, 24, 25). From repeated and detailed single-cell recordings by both fiber photometry and microendoscopy, we found that orexin neurons became essentially quiescent prior to the transition from NREM sleep to REM sleep (Figs. 1 and 2 and *SI Appendix*, Fig. S3). While these findings suggest that the activity dynamics of orexin neurons during NREM sleep play a regulatory role in the transition from NREM sleep to REM sleep (NREM–REM sleep transition), optogenetic inhibition of orexin neurons was previously shown to only increase NREM sleep time (42–44). Thus, we tested whether optogenetic silencing of orexin neurons increased NREM–REM sleep

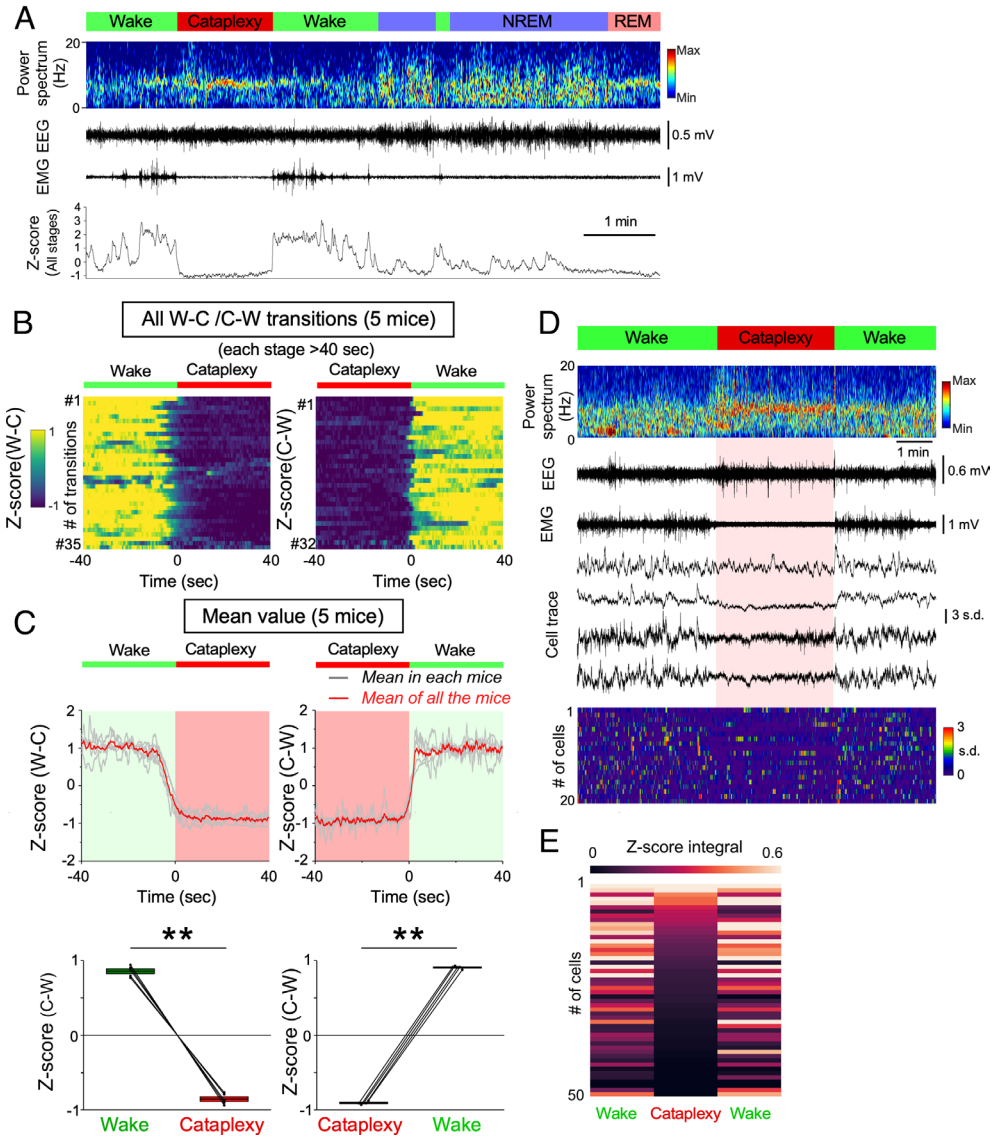

Fig. 5. Activity of orexin neurons during cataplexy in *prepro-orexin* knockout [*orexin-Flp (KI/KI)*] mice. (*A*) Representative trace of orexin neuron activity during cataplexy as measured by fiber photometry. (*B*) Activity of orexin neurons of all the state transitions (wake to cataplexy and cataplexy to wake, each stage > 40 s), measured from 24-h recordings in N = 5 mice. (*C*, *Top*) Mean Z-score of all the transitions in each individual mouse (gray); mean Z-score of all the N = 5 mice (red). (*C*, *Bottom*) Summary of orexin neuron activity of all the mice (wake to cataplexy and cataplexy to wake) shown as Z-scores. (*D*) Representative traces of the activity of 20 orexin neurons during cataplexy measured using nVista. (*E*) Summary of orexin neuron activity during transitions between wake and cataplexy for N = 50 orexin neurons from N = 3 mice. Values are the mean ± SEM. $^{**}P < 0.01$. Statistical analyses are shown in *SI Appendix*, Table S1. C, cataplexy; W, wakefulness.

transitions. The neural silencer Archaerhodopsin-T (ArchT) fused with enhanced green fluorescent protein (EGFP) was exclusively expressed in orexin neurons following bilateral injection of AAV9-TetO-ArchT-EGFP into the LHA of *orexin-tTA* mice (Fig. 6 *A* and *B*). Expression of ArchT and optogenetic inhibition was validated by immunostaining and patch-clamp recordings, respectively (*SI Appendix*, Fig. S7).

One-h continuous inhibition of orexin neurons during Zeitgeber time (ZT) seven to eight significantly decreased the time in wakefulness and increased the time in NREM and REM sleep compared to baseline (Fig. 6 *C*–*E*). Importantly, we found that the transition ratio (REM bouts/NREM bouts) and the cumulative probability of transitioning from NREM sleep to REM sleep significantly increased (Fig. 6*H*) whereas these parameters from NREM sleep to wakefulness decreased (Fig. 6*G*), suggesting a disproportionate increase in the transition from NREM sleep to REM sleep when orexin neurons are inhibited. EGFP-expressing control mice did not show any significant change in these parameters (*SI Appendix*, Fig. S8 *A*–*E*). Optogenetic inhibition of orexin neurons also significantly increased the hypersynchronous paroxysmal theta (HSPT) bursts that are characteristic of REM sleep and cataplexy in other mouse models of narcolepsy (45, 46), indicating that optogenetic inhibition of orexin neurons was successful (Fig. 6 *D* and *F*). Spectral analysis showed that EEG power was affected, but the difference was not significant (*SI Appendix*, Fig. S9*A*). Moreover, to test whether intermittent orexin neuron activation during NREM sleep prevented the NREM–REM sleep transition, we also conducted an intermittent stimulation of orexin neurons (four times/min) for 1 h at ZT6-7 using bigenic *orexin-tTA; TetO-ChR2* (47) mice. This intermittent stimulation protocol reduced the transition ratio and cumulative probability of the NREM–REM sleep transition, without reducing NREM and REM sleep duration (*SI Appendix*, Fig. S10 *A*–*H*). Given that only the activity during NREM sleep is thought to contribute to the subsequent transition from NREM sleep, these results also support the idea that the intermittent activity of orexin neurons

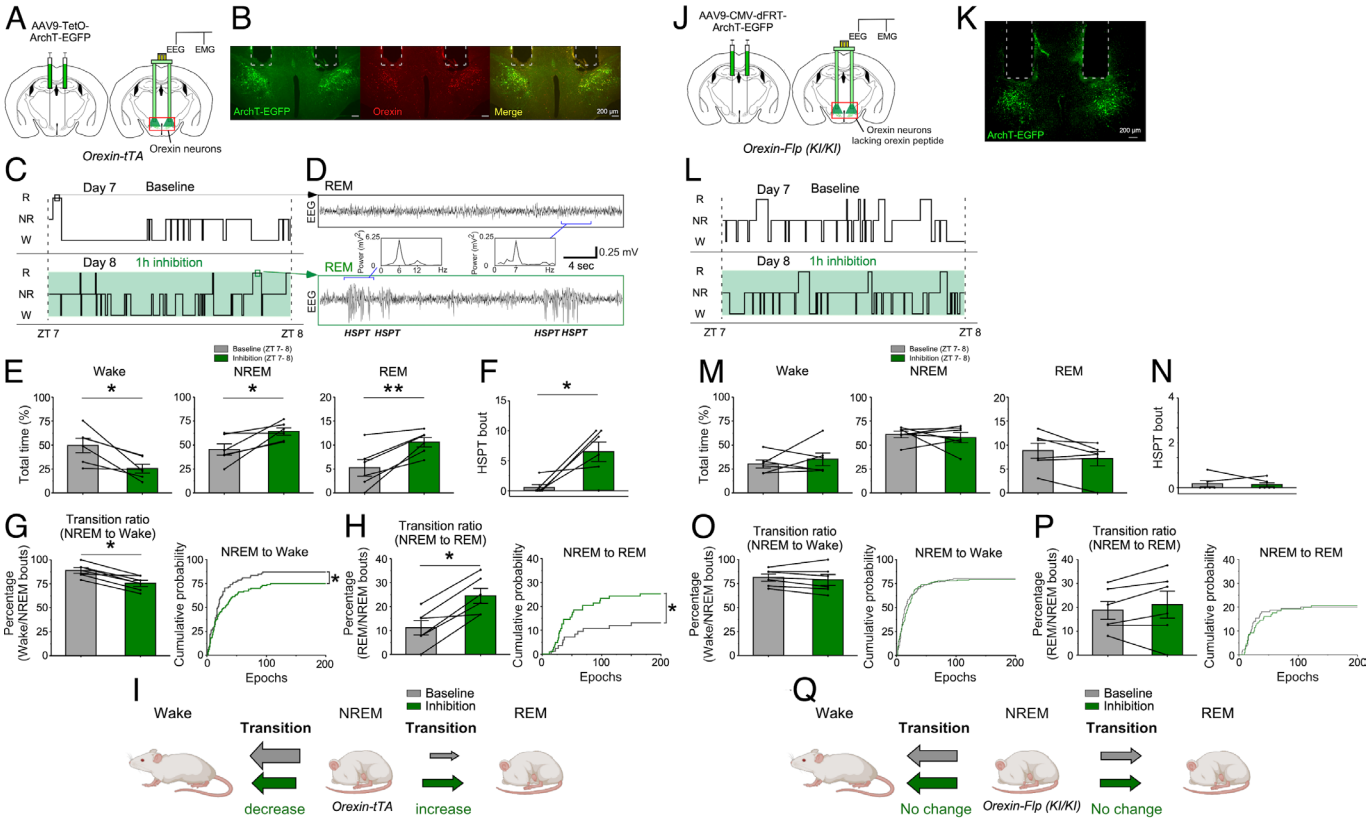

Fig. 6. Effects of optogenetic inhibition of orexin neurons on NREM–REM transitions in mice with or without orexin peptide expression. (*A*) Schematics of ArchT-EGFP expression in orexin neurons in *orexin-tTA* mice (*Left*) and implantation of bilateral optic fibers with EEG/EMG recordings (*Right*). (*B*) Immunohistochemical confirmation of ArchT-EGFP expression in orexin neurons in *orexin-tTA* mice (N = 6 mice). Dashed lines at the top of each image indicate the edge of the optic fiber. (*C*) Hypnogram (ZT7-8) during baseline (*Upper*) and optogenetic inhibition (*Lower*). (*D*) Representative EEG during REM sleep at baseline (*Upper*) and during optogenetic inhibition (*Lower*). *Insets* are EEG spectra of the indicated epochs. Note episodes of hypersynchronous paroxysmal theta (HSPT) in the EEG. (*E*) Total time in each vigilance state during baseline (gray) and optogenetic inhibition (green). (*F*) The number of HSPT bouts during baseline (gray) and optogenetic inhibition (green) in orexin neurons from *orexin-tTA* mice. (*G*) Optogenetic inhibition of orexin neurons decreases the transition ratio (*Left*) and cumulative probability (*Right*) for the NREM sleep to Wake transition in *orexin-tTA* mice. (*H*) Optogenetic inhibition of orexin neurons increases the transition ratio (*Left*) and cumulative probability (*Right*) for the NREM to REM sleep transition in mice expressing the orexin peptides (*orexin-tTA mice*). (*I*) Schematic summarizing the effect of optogenetic inhibition of orexin neurons in *orexin-tTA* mice. (*J*) Schematics of ArchT-EGFP expression in orexin neurons from *orexin-Flp (KI/KI)* mice which lack orexin peptides (N = 6 mice). (*K*) Histochemical confirmation of ArchT-EGFP expression in *orexin-Flp (KI/KI)* mice; dashed lines indicate the location of the optic fiber. (*L*) Hypnogram (ZT7-8) during baseline (*Upper*) and optogenetic inhibition (*Lower*). (*M*) Total time in each vigilance state during baseline (gray) and optogenetic inhibition (green) of orexin neurons in *orexin-Flp (KI/KI)* mice. (*N*) The number of HSPT bouts during baseline (gray) and optogenetic inhibition (green). (*O*) Transition ratio (*Left*) and cumulative probability (*Right*) for the transition from NREM sleep to Wake. (*P*) Transition ratio (*Left*) and cumulative probability (*Right*) for the transition from NREM to REM sleep. (*Q*) Schematic summarizing the absence of any effect of optogenetic inhibition of orexin neurons in *orexin-Flp (KI/KI)* mice. Values are the mean ± SEM. **P* < 0.05, ***P* < 0.01. Statistical analyses are in *SI Appendix*, Table S1. HSPT, Hypersynchronous paroxysmal theta burst.

during NREM sleep prevents the NREM–REM sleep transition, whereas a decrease in orexin neuron activity during NREM sleep promotes the NREM–REM sleep transition (Fig. 6*I*).

Orexin neurons release not only orexin peptides but also other neurotransmitters such as glutamate and dynorphin. Thus, the role of orexin peptides in the regulation of NREM–REM sleep transitions by orexin neurons remains unknown. To address this question, AAV9-CMV-dFRT-ArchT-EGFP was bilaterally injected into the LHA of *orexin-Flp (KI/KI)* mice and orexin neurons that lacked orexin peptides were subjected to optogenetic inhibition (Fig. 6 *J* and *K*). The exclusive expression of ArchT-EGFP in orexin neurons was confirmed using heterozygous *orexin-Flp (KI/-)* mice and functional expression of ArchT in orexin neurons lacking orexin peptides was confirmed by patch-clamp recordings (*SI Appendix*, Fig. S11 *A–G*). In contrast to inhibiting orexin neurons that express orexin peptides in *orexin-tTA* mice, inhibition of orexin neurons lacking orexin peptides in *orexin-Flp (KI/KI)* mice did not affect total time spent in each state, the transition ratio, HSPT bouts (Fig. 6 *L–Q*) or the EEG spectrum (*SI Appendix*, Fig. S9*B*). GFP-expressing control mice did not show any significant change in these parameters (*SI Appendix*, Fig. S8 *F–J*). These results suggest that the orexin peptides are a critical component in the regulation of NREM–REM sleep transitions by orexin neuron activity during NREM sleep.

Orexin Neuron Activity during REM Sleep Affects Subsequent REM Sleep Architecture and Cataplexy. The results from fiber photometry and continuous optogenetic inhibition suggest an inhibitory role for orexin neuron activity in NREM–REM sleep transitions. However, the significance of orexin neuron activity during REM sleep, which is lower in narcolepsy model mice (Figs. 1*F*, 2*F*, and *SI Appendix*, Fig. S3*G* vs. 3*F* and 4*F*), remains unclear. It has long been thought that orexin neurons have REM sleep–suppressing activity (8, 17, 25). Thus, we hypothesized that orexin neuron activity during REM sleep is involved in the increased REM sleep characteristic of narcolepsy. To test this hypothesis, we took advantage of previous studies in which published figures implied that REM sleep is increased not only during the dark period, but also during the latter portion (last 4 h) of the light period in narcolepsy model mice compared to wild-type mice (4, 19). We confirmed this observation in narcoleptic *orexin-Flp (KI/KI)* mice compared to both *orexin-tTA* mice and wild-type mice. In *orexin-Flp (KI/KI)* mice, REM sleep during

ZT8-12 and during ZT12-18 is significantly increased compared to phenotypically normal *orexin-tTA* mice (Fig. 7 *A* and *B*) and wild-type mice (6.7 ± 0.4% vs. 7.9 ± 0.4% (not significant) during ZT 3 to 8, 8.4 ± 0.6% vs. 6.2 ± 0.3% ($P < 0.01$) during ZT8-12, and 4.9 ± 0.8% vs. 1.7 ± 0.3% ($P < 0.01$) during ZT 12 to 18, *SI Appendix*, Table S1).

Since sleep disruption at night increases sleepiness during the daytime in humans, we similarly hypothesized that orexin neuron activity during REM sleep in the preceding period (ZT3-8) affects the increase in subsequent REM sleep from ZT8-12, as shown in narcoleptic mice (Fig. 7 *A* and *B*). To test this, we performed state-dependent optogenetic inhibition of orexin neurons from ZT3 to ZT8 in *orexin-tTA* and analyzed the effect on vigilance states during the subsequent 10 h (light period: ZT8-12; dark period: ZT12-18) after inhibition had been terminated. Sleep/wakefulness states were automatically discriminated using

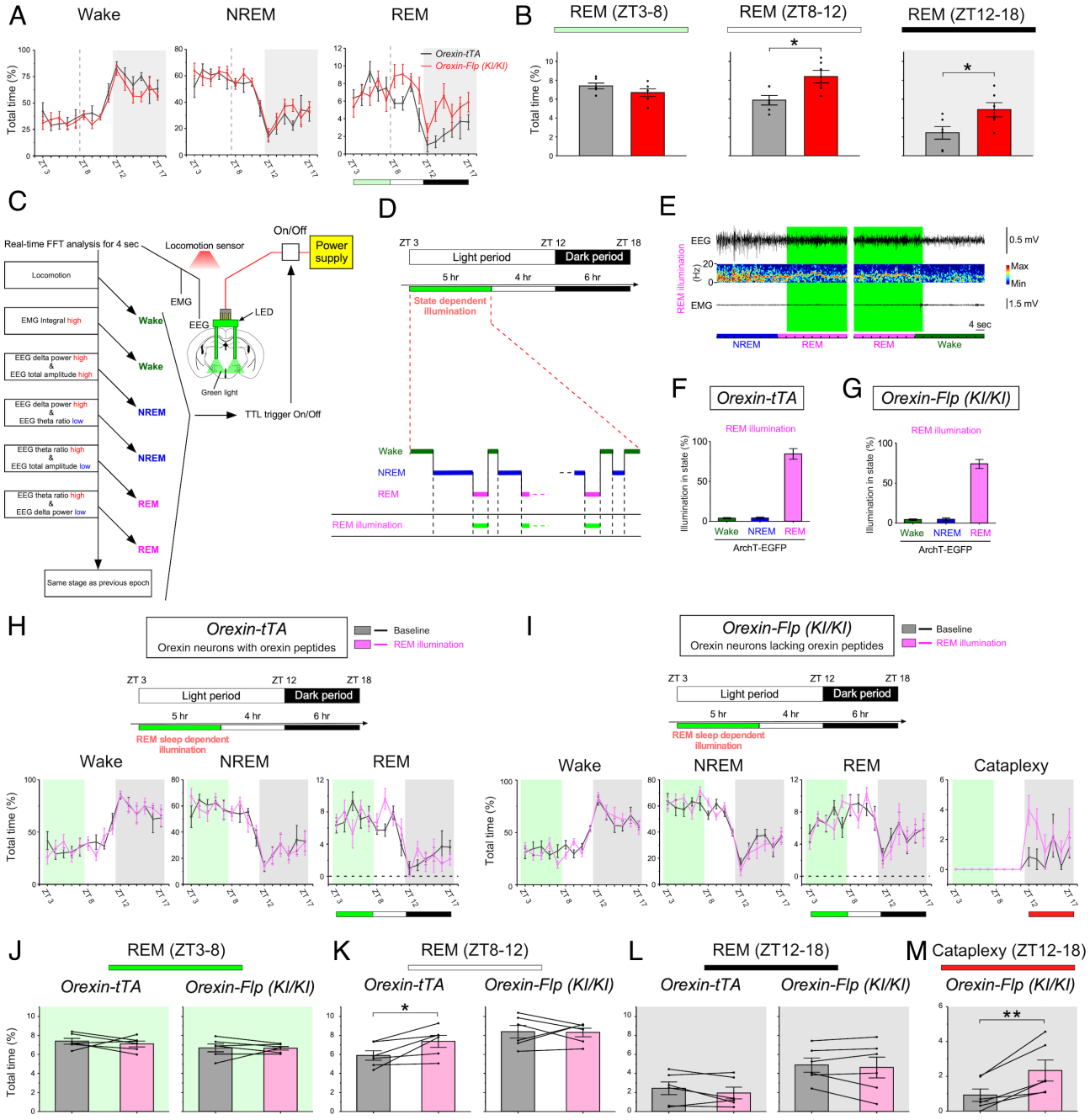

Fig. 7. REM sleep state–dependent inhibition of orexin neurons with and without orexin peptides regulates subsequent REM sleep architecture and cataplexy. (*A* and *B*) Line graphs showing the time spent in each vigilance state (*A*) and bar graphs summarizing the time spent in REM sleep during each time period (*B*) in *orexin-tTA* mice (black, N = 6 mice) and *prepro-orexin* knockout mice [*orexin-Flp (KI/KI)*; red, N = 6 mice]. (*C*) Decision tree algorithm for real-time vigilance-state determination using EEG, EMG, and locomotion. (*D* and *E*) Photoillumination of orexin neurons expressing ArchT-EGFP during REM sleep results in REM sleep state–dependent inhibition. (*F* and *G*) Bar graphs indicating the illumination "cover ratio" for REM sleep in *orexin-tTA* mice (*F*) and *prepro-orexin* knockout mice [*orexin-Flp (KI/KI)*; *G*]. (*H* and *I*) Line graphs showing the effects of REM sleep state–dependent inhibition on the time spent in each vigilance state during state-dependent illumination (ZT3-8), the subsequent light period (ZT8-12), and the subsequent dark period (ZT12-18) *in orexin-tTA* mice (*H*) and *prepro-orexin* knockout [*orexin-Flp (KI/KI)*) mice (*I*)]. (*J–M*) Bar graphs showing the effects of REM sleep state–dependent inhibition on the time spent in REM sleep and cataplexy at each time period (ZT3-8, ZT8-12, and ZT12-18) *in orexin-tTA* mice (*Left* in *J–L*) and *prepro-orexin* knockout mice [*orexin-Flp (KI/KI)*; *Right* in *J–L* and *M*). Statistics for other vigilance states during each time period are described in *SI Appendix*, Table S1. Data are the mean ± SEM. *$P < 0.05$, **$P < 0.01$. Statistical analyses are shown in *SI Appendix*, Table S1. FFT, fast Fourier transform; TTL, transistor–transistor logic.

EEG, EMG, and locomotor activity, which enabled immediate closed loop-triggering of photoillumination during specific states (48) (Fig. 7 *C–E* and *SI Appendix*, Fig. S14 *A* and *B*). REM sleep state–dependent triggering of photoillumination spanned 84.3 ± 6.7% of REM sleep (total time) with little illumination during nontarget states (Fig. 7*F*). The time spent in vigilance states under REM sleep state–dependent inhibition (ZT3-8) did not differ from baseline (Fig. 7 *H* and *J*, *Left*) or yoked (joined together) controls in which the subjected mice (yoked controls) received optogenetic inhibition whenever the matched mice showed REM sleep (*SI Appendix*, Fig. S12 *A–C*, *E*, and *G*, *Left*). However, the time spent in subsequent REM sleep (ZT8-12) in *orexin-tTA* mice significantly increased compared to baseline (Fig. 7*H* and *K*, *Left*) and yoked control (*SI Appendix*, Fig. S12 *E* and *H*, *Left*), but not in the EGFP-expressing control mice (*SI Appendix*, Fig. S13 *A–C* and *H*, *Left*). After NREM sleep–specific inhibition (*SI Appendix*, Fig. S14 *A–C*), a significant reduction in NREM sleep and an increase in wakefulness during the dark period were also observed (*SI Appendix*, Fig. S14 *E* and *F*). In contrast, wakefulness-specific inhibition (*SI Appendix*, Fig. S14 *A–C*) did not affect vigilance states (*SI Appendix*, Fig. S14 *G* and *H*). Thus, the inhibition of orexin neuron activity during REM sleep at a time of day when REM sleep is normally high caused a subsequent overexpression of REM sleep. Therefore, it produced a REM sleep increase in *orexin-tTA* mice at ZT8-12, but not at ZT3-8, similar to the REM sleep structure at ZT3-8 and ZT8-12 in narcolepsy.

These results encouraged us to hypothesize that REM sleep state–dependent inhibition of orexin neurons lacking orexin peptides might exacerbate subsequent cataplexy in narcolepsy model mice. Orexin neurons in *orexin-Flp (KI/KI)* mice which lack orexin peptides were state-dependently inhibited during REM sleep from ZT3-8. REM sleep state–dependent triggering of photoillumination spanned 74.0 ± 5.6% of REM sleep (total time) with little illumination during nontarget states (Fig. 7*G*). Time in vigilance states did not differ among time periods (Fig. 7 *I* and *J–L*, *Right*). However, time in cataplexy in *orexin-Flp (KI/KI)* mice significantly increased during the dark period after REM sleep state–dependent inhibition compared to baseline (Fig. 7 *I* and *M*) and yoked controls (*SI Appendix*, Fig. S12 *D*, *F*, and *J*), but not in the GFP-expressing control mice (*SI Appendix*, Fig. S13 *D–F* and *J*). Thus, our results suggest that orexin neuron activity during preceding REM sleep has an inhibitory role on subsequent cataplexy during the dark period. Taken together, these results show that the activity dynamics of orexin neurons during NREM and REM sleep are involved in the abnormal REM sleep architecture in narcolepsy.

Discussion

Here, we revealed the activity dynamics and physiological roles of orexin neurons during sleep in both *orexin-tTA* mice and *orexin-Flp (KI/-)* mice and in *orexin-Flp (KI/KI)* narcolepsy model mice (*SI Appendix*, Fig. S15). Orexin neurons in both *orexin-tTA* mice and *orexin-Flp (KI/-)* mice showed intermittent and synchronous activity in NREM sleep but were essentially quiescent before transitions to REM sleep (tNR), suggesting that orexin neuron activity during NREM sleep is involved in the regulation of the REM sleep transition. This role was also confirmed by the disproportionate increase or decrease in REM sleep transitions by continuous inhibition or intermittent activation, respectively, of orexin neurons in *orexin-tTA* mice. A subpopulation of orexin neurons showed weak activity during REM sleep. REM sleep state–dependent inhibition revealed that orexin neuron activity during the preceding REM sleep has an inhibitory role in subsequent REM sleep architecture in *orexin-tTA* mice and cataplexy in *orexin-Flp (KI/KI)* mice. Although the role of orexin neurons in promoting wakefulness is well established (20–24), our results revealed that the loss of the normal roles for orexin neurons during sleep as well as during wakefulness are involved in the REM sleep–related symptomatology of narcolepsy.

Orexin neurons showed different activity patterns between NREM sleep and REM sleep, suggesting that these cells receive distinct neural regulation during NREM vs. REM sleep. Li et al. reported that hyperexcitable orexin neurons drive sleep fragmentation during aging through intermittent activity during NREM sleep (33). The intermittent synchronous activity during NREM sleep might be generated intrinsically by burst activity from orexin neurons. In slice patch-clamp recordings, some orexin neurons showed intermittent burst activity (49). We also reported that orexin neurons form a positive-feedback loop both directly and indirectly (50). These neural mechanisms might form the basis of synchronous activity and this synchronous activity in NREM sleep could be resisted by inhibitory inputs from sleep-promoting neurons such as the preoptic area during NREM sleep (51, 52).

This intermittent activity during NREM sleep may push the brain state toward wakefulness and thus may contribute to the generation of a "microarousal"-like state in NREM sleep, which is often observed in rodents. Microarousal has also been associated with the activity of orexin neurons and might help animals stay alert during NREM sleep for survival. This activity inhibits NREM–REM sleep transitions and, importantly, orexin peptides appear to be indispensable for this inhibitory role. Loss of this function could be one of neural mechanisms behind the frequent transitions in narcolepsy (17, 19, 25, 36, 53–55). Weber et al. (7) reported a gating role for GABAergic neurons in the ventrolateral periaqueductal gray (vlPAG) in the transition from NREM sleep to REM sleep. Orexin neurons are known to project to vlPAG (56) and thus may interact to suppress the transition to REM sleep.

We also observed activity in a subpopulation of orexin neurons during REM sleep. However, this REM activity was diminished in orexin neurons from *orexin-Flp (KI/KI)* mice which lack the orexin peptides, suggesting that the orexin peptides contributed to the generation of orexin neuron activity during REM sleep. We previously reported impaired activity of orexin neurons that lacked the orexin peptides when recorded by patch-clamp electrophysiology (36). Orexin neuron activity during REM sleep may be more susceptible to impairment due to loss of orexin peptides than other states because orexin neurons exhibit a continuous, low activity during REM sleep by a smaller population of cells. Moreover, we found that orexin neuron activity was suppressed in cataplexy and appeared similar to orexin neuron activity during REM sleep in *orexin-Flp (KI/KI)* mice. It has previously been reported that other wake-promoting neurons, such as histaminergic neurons in the tuberomammillary nucleus (TMN), are highly active in cataplexy as well as wakefulness (57). The inverse activities between orexin neurons and other wake-promoting neurons during cataplexy could underlie the neuronal basis of cataplexy or sleep paralysis with "sleep-like" muscle atonia under "wakefulness-like" consciousness.

Orexin signaling during REM sleep suppressed an increase in subsequent REM sleep in phenotypically normal *orexin-tTA* mice and cataplexy in *orexin-Flp (KI/KI)* narcolepsy model mice. This observation supports the idea that orexin signaling during REM sleep relieves/reduces the requirement for REM sleep. The previous findings that orexin peptides strongly inhibit REM sleep and that REM sleep pressure accumulates in narcolepsy (25) are consistent with our present results. Interestingly, 48 h of REM sleep

deprivation has been found to increase subsequent cataplexy in narcoleptic mice (4). Optogenetic inhibition of orexin signaling during REM sleep in *orexin-Flp (KI/KI)* mice replicated this phenomenon at the neural circuitry level. Thus, orexin signaling in REM sleep could be one of the neural mechanisms regulating REM sleep requirements or pressure. The exacerbation of cataplexy by REM sleep state–dependent inhibition of orexin neurons that lack orexin peptides also suggests colocalized neurotransmitters, such as glutamate, may play a role in the inhibition of cataplexy. In this regard, mice lacking orexin neurons generally exhibit more severe narcolepsy symptoms than *prepro-orexin* knockout or orexin receptor knockout mice (24, 54).

State-dependent inhibition of orexin neurons affected subsequent vigilance states (ZT8-12) but not during inhibition (ZT3-8). A possible explanation for this could be that the accuracy of state-dependent inhibition was ~90% and not 100%. The algorithm underlying our closed-loop photoillumination system requires one 4-s epoch to determine the vigilance state, which means that orexin peptides can be released during the initial 4 s. It is also known that orexin peptides act via volume transmission. Trace levels of orexin peptides in the cerebrospinal fluid released by such "leak activity" or by activity during other states might weaken the effect of state-dependent inhibition. In fact, trace levels of orexin peptides in the basal forebrain were reported to remain similarly higher during both NREM sleep and wakefulness, but reduced during REM sleep (58). Alternatively, optogenetic inhibition may be followed by rebound neuronal hyperactivity due to hyperpolarization-induced current (H current) in orexin neurons (49). This rebound activity associated with intermittent photoinhibition at each state may weaken the effect of state-dependent inhibition. These were considered to be methodological limitations of state-dependent inhibition.

As another possibility, in narcolepsy, REM sleep is greater during the last 4 h (ZT8-12) of the light period compared to WT as shown in the Results (Fig. 7 *A* and *B*), but not during the typical sleep period (ZT3-8). Thus, it is possible that state-dependent inhibition from ZT3-8 did not increase REM sleep during this typical sleep period (ZT3-8) when relatively more REM sleep normally occurs but increases REM sleep during the latter part of the light period (ZT8-12) when a relatively small amount of REM sleep normally occurs. It is also reasonable that "the rebound REM as cataplexy" occurs in the dark period with a 4-h delay because wakefulness (which is dominant during the dark period) is necessary for the occurrence of cataplexy.

Another limitation is that we could not record cataplexy in all five *orexin-Flp (KI/KI)* mice in which microendoscopy recording was conducted, but recorded cataplexy only in three mice that had REM-active orexin neurons. This was because, due to the limited recording period for microendoscopy experiments, it was difficult to observe a spontaneously occurring rare event such as cataplexy during such recordings, particularly given the preceding 40-s wakefulness criterion required by the international consensus. Although we observed the activity of orexin neurons during REM sleep and cataplexy, the number of neurons recorded during both REM sleep and cataplexy is relatively small. Thus, to clarify this point, further studies may be warranted. Moreover, although we used chocolate to induce cataplexy, it is unknown whether the circuit underlying chocolate-induced cataplexy is the same as for spontaneous cataplexy.

Here, we identified the roles for orexin neuron activity dynamics in NREM and REM sleep using mice with and without orexin peptides. Taken together, our findings provide important clues not only for the development of treatments for narcolepsy, but also for understanding the neural regulatory mechanisms underlying sleep/wakefulness states.

Materials and Methods

A full description of experimental materials and methods are in *SI Appendix, Supplementary Materials and Methods*.

Animals. All experimental protocols involving the use of mice were approved by the Institutional Animal Care and Use Committees, Research Institute of Environmental Medicine, Nagoya University, Japan (#19232 and #19268) and SRI International (#01026). All efforts were made to reduce the number of mice used and to minimize the pain and suffering of mice.

Adeno-Associated Viral (AAV) Production and Injection. AAV Helper-Free System (Agilent Technologies, Inc., Santa Clara, CA, USA), AAV vectors were used to produce and purify. HEK293 cells were transfected with pAAV vector plasmid that included a gene of interest, pHelper and pAAV-RC using a standard calcium phosphate method.

For AAV injection, mice were anesthetized with isoflurane (Wako Pure Chemical Industries) anesthesia (< 2%) and fixed in a stereotaxic frame (David Kopf Instruments). Using injectors (BJ-110; BEX CO, Ltd., Itabashi, Tokyo, Japan or Nanoject III; Drummond Scientific Company, Broomall, PA, USA), AAV was injected into the LHA

EEG/EMG Surgery. Two screws (U-1430-01, Wilco, Yokohama, Japan) were implanted on the skull (AP = +0.5 to 1.0 mm; ML = −0.5 to −1.0 mm and AP = −2.5 to 3.0 mm; ML = −2.5 to −3.0 mm) to record EEG, and two stainless steel wires (209-4811, RS PRO, Yokohama, Japan) were inserted on either side of the nuchal muscle to record EMG.

In Vivo Ca^{2+} Imaging Using nVista. More than 3 wk after AAV injection, a GRIN lens (length of 8.4 mm, diameter of 1 mm, Inscopix, Palo Alto, CA, USA) was implanted above the LHA (AP = −1.4 mm; ML = +0.9 mm; DV = −4.6 to 5.0 mm). At the same time, an acrylic bar for head fixation was attached to the skull using Super-bond (Super-bond C&B, Sun Medical, Moriyama, Japan). More than 1 wk after implantation, the mouse was attached to a stereotaxic frame using the acrylic bar. A baseplate (Inscopix, Palo Alto, CA) was attached using dental cement (REPAIRSIN, GC) to hold a microendoscope (nVista, Inscopix). Then the microendoscope was attached to the head to monitor GCaMP6s fluorescence through the implanted GRIN lens. Images were acquired at 10 to 20 frames/s with 0.2 to 1.1 mW of LED light (475 nm) using nVista HD Acquisition Software (version 3; Inscopix). All images were processed using Mosaic Software (version 2.0; Inscopix) and Inscopix Data Processing Software (IDPS, version 1.6.1, Inscopix).

Optogenetic Inhibition/Stimulation and Vigilance State–Dependent Illumination. At least 3 wk after AAV injection, LED cannulae (fiber diameter 500 μm, fiber length 5 mm, bilateral, 525 nm, 3.2 mW; Bio Research Center) were implanted (AP = −1.4 mm; ML = ±0.9 mm; DV = −4.5 mm) during EEG/EMG surgery. LED cannulae (fiber diameter 400 μm, fiber length 5 mm, bilateral; Kyocera Corporation, Japan) were implanted (AP = −1.4 mm; ML = ±0.9 mm; DV = −4.5 mm). The vigilance state for each epoch was automatically defined in real time using the following decision tree algorithm by SleepSignRecorder (Kissei Comtec). Photo illumination was triggered by Transistor-Transistor Logic (TTL) output from SleepSignRecorder. After the experiments, the cover ratio of illumination for each vigilance state was calculated by comparison with offline determination.

Electrophysiology. Brains were rapidly isolated and chilled in ice-cold bubbled (95% O_2 and 5% CO_2) cutting solution. Coronal brain sections of 300-μm thickness were made using a vibratome (VT-1200S, Leica). The slices were incubated in a bubbled (95% O_2 and 5% CO_2) bath solution. electrophysiological properties of the cells were continuously monitored using the Axopatch 200B amplifier (Axon Instruments, Molecular Devices, Sunnyvale, CA). Patch-clamp data were recorded using an analog-to-digital (AD) converter (Digidata 1550A, Molecular Devices) and pClamp 10.7 software (Molecular Devices).

Statistical Analysis. Statistical analyses were performed using OriginPro 2020 software (LightStone, Tokyo, Japan), easy R (1.37), or Python (3.7). All data are presented as the mean ± SEM. Details of the statistical tests are described in *SI Appendix*, Table S1. Significant differences were set at $P < 0.05$.

Data, Materials, and Software Availability. All study data are included in the article and/or supporting information.

ACKNOWLEDGMENTS. We thank Dr. Nomoto and Dr. Inokuchi at the University of Toyama for introducing the NMF clustering analysis. We thank S. Tsukamoto, S. Nasu, E. Imoto, and T. Miyazaki for technical assistance and helpful support. We thank the Center for Animal Research and Education at Nagoya University for breeding animals. This work was supported by JST CREST (JPMJCR1656), AMED-CREST (JP20GM1310007), Mitsubishi foundation, Senshin-iyaku foundation and Kao Kenkokagaku foundation to A.Y., KAKENHI grants (19J22270) to H.I., (21K20688 and 22K15225) to Y.M., and (21H02526, 20KK0177 and 18H02477) to D.O., (26293046, 26640041, 16H01271, 17H05563, 18H05124, 18KK0223 and 18H02523) to A.Y. and NIH R01 NS098813 and R01 NS103529 to T.S.K.

Author affiliations: [a]Department of Neuroscience II, Research Institute of Environmental Medicine, Nagoya University, Nagoya 464-8601, Japan; [b]Department of Neural Regulation, Nagoya University Graduate School of Medicine, Nagoya 466-8550, Japan; [c]Japan Society for the Promotion of Science Research Fellowship for Young Scientists, Tokyo 102-0083, Japan; [d]Center for Neuroscience, Biosciences Division, SRI International, Menlo Park, CA 94025; [e]Chinese Institute for Brain Research, Beijing 102206, China; [f]National Institute for Physiological Sciences, Aichi 444-8585, Japan; [g]National Institutes of Natural Sciences, Aichi 444-8585, Japan; and [h]Division of Brain Sciences Institute for Advanced Medical Research, Keio University School of Medicine, Tokyo 160-8582, Japan

1. A. Rechtschaffen, B. M. Bergmann, M. A. Gilliland, K. Bauer, Effects of method, duration, and sleep stage on rebounds from sleep deprivation in the rat. *Sleep* **22**, 11–31 (1999).
2. J. A. Horne, REM sleep - by default? *Neurosci. Biobehav. Rev.* **24**, 777–797 (2000).
3. H. Feng *et al.*, Orexin signaling modulates synchronized excitation in the sublaterodorsal tegmental nucleus to stabilize REM sleep. *Nat. Commun.* **11**, 3661 (2020).
4. A. Roman, S. Meftah, S. Arthaud, P. H. Luppi, C. Peyron, The inappropriate occurrence of rapid eye movement sleep in narcolepsy is not due to a defect in homeostatic regulation of rapid eye movement sleep. *Sleep* **41**, zsy046 (2018).
5. S. Arthaud, P. A. Libourel, P. H. Luppi, C. Peyron, Insights into paradoxical (REM) sleep homeostatic regulation in mice using an innovative automated sleep deprivation method. *Sleep* **43**, zsaa003 (2020).
6. E. Aserinsky, N. Kleitman, Regularly occurring periods of eye motility, and concomitant phenomena, during sleep. *Science* **118**, 273–274 (1953).
7. F. Weber *et al.*, Regulation of REM and Non-REM sleep by periaqueductal GABAergic neurons. *Nat. Commun.* **9**, 354 (2018).
8. S. H. Park, F. Weber, Neural and homeostatic regulation of REM sleep. *Front. Psychol.* **11**, 1662 (2020).
9. E. Hasegawa *et al.*, Rapid eye movement sleep is initiated by basolateral amygdala dopamine signaling in mice. *Science* **375**, 994–1000 (2022).
10. A. K. Barnes, R. Koul-Tiwari, J. M. Garner, P. A. Geist, S. Datta, Activation of brain-derived neurotrophic factor-tropomyosin receptor kinase B signaling in the pedunculopontine tegmental nucleus: a novel mechanism for the homeostatic regulation of rapid eye movement sleep. *J. Neurochem.* **141**, 111–123 (2017).
11. S. Datta, C. M. Knapp, R. Koul-Tiwari, A. Barnes, The homeostatic regulation of REM sleep: A role for localized expression of brain-derived neurotrophic factor in the brainstem. *Behav. Brain Res.* **292**, 381–392 (2015).
12. Y. Mukai, A. Yamanaka, Functional roles of REM sleep. *Neurosci. Res.*, 10.1016/j.neures.2022.12.009 (2022).
13. L. de Lecea *et al.*, The hypocretins: Hypothalamus-specific peptides with neuroexcitatory activity. *Proc. Natl. Acad. Sci. U.S.A.* **95**, 322–327 (1998).
14. T. Sakurai *et al.*, Orexins and orexin receptors: A family of hypothalamic neuropeptides and G protein-coupled receptors that regulate feeding behavior. *Cell* **92**, 573–585 (1998).
15. C. Peyron *et al.*, A mutation in a case of early onset narcolepsy and a generalized absence of hypocretin peptides in human narcoleptic brains. *Nat. Med.* **6**, 991–997 (2000).
16. T. C. Thannickal *et al.*, Reduced number of hypocretin neurons in human narcolepsy. *Neuron* **27**, 469–474 (2000).
17. R. M. Chemelli *et al.*, Narcolepsy in orexin knockout mice: molecular genetics of sleep regulation. *Cell* **98**, 437–451 (1999).
18. L. Lin *et al.*, The sleep disorder canine narcolepsy is caused by a mutation in the hypocretin (orexin) receptor 2 gene. *Cell* **98**, 365–376 (1999).
19. T. Mochizuki *et al.*, Behavioral state instability in orexin knock-out mice. *J. Neurosci.* **24**, 6291–6300 (2004).
20. C. R. Burgess, T. E. Scammell, Narcolepsy: Neural mechanisms of sleepiness and cataplexy. *J. Neurosci.* **32**, 12305–12311 (2012).
21. T. E. Scammell, Narcolepsy. *N Engl. J. Med.* **373**, 2654–2662 (2015).
22. S. Pintwala, J. Peever, Circuit mechanisms of sleepiness and cataplexy in narcolepsy. *Curr. Opin. Neurobiol.* **44**, 50–58 (2017).
23. C. L. A. Bassetti *et al.*, Narcolepsy – clinical spectrum, aetiopathophysiology, diagnosis and treatment. *Nat. Rev. Neurol.* **15**, 519–539 (2019).
24. C. E. Mahoney, A. Cogswell, I. J. Koralnik, T. E. Scammell, The neurobiological basis of narcolepsy. *Nat. Rev. Neurosci.* **20**, 83–93 (2019).
25. M. H. Hansen, B. R. Kornum, P. Jennum, Sleep-wake stability in narcolepsy patients with normal, low and unmeasurable hypocretin levels. *Sleep Med.* **34**, 1–6 (2017).
26. L. I. Kiyashchenko, B. Y. Mileykovskiy, Y. Y. Lai, J. M. Siegel, Increased and decreased muscle tone with orexin (hypocretin) microinjections in the locus coeruleus and pontine inhibitory area. *J. Neurophysiol.* **85**, 2008–2016 (2001).
27. L. Verret *et al.*, A role of melanin-concentrating hormone producing neurons in the central regulation of paradoxical sleep. *BMC Neurosci.* **4**, 19 (2003).
28. M. Modirrousta, L. Mainville, B. E. Jones, Orexin and MCH neurons express c-Fos differently after sleep deprivation vs. recovery and bear different adrenergic receptors. *Eur. J. Neurosci.* **21**, 2807–2816 (2005).
29. M. G. Lee, O. K. Hassani, B. E. Jones, Discharge of identified orexin/hypocretin neurons across the sleep-waking cycle. *J. Neurosci.* **25**, 6716–6720 (2005).
30. B. Y. Mileykovskiy, L. I. Kiyashchenko, J. M. Siegel, Behavioral correlates of activity in identified hypocretin/orexin neurons. *Neuron* **46**, 787–798 (2005).
31. K. Takahashi, J. S. Lin, K. Sakai, Neuronal activity of orexin and non-orexin waking-active neurons during wake-sleep states in the mouse. *Neuroscience* **153**, 860–870 (2008).
32. I. A. Azeez, F. Del Gallo, L. Cristino, M. Bentivoglio, Daily fluctuation of orexin neuron activity and wiring: The challenge of "Chronoconnectivity". *Front. Pharmacol.* **9**, 1061 (2018).
33. S. B. Li *et al.*, Hyperexcitable arousal circuits drive sleep instability during aging. *Science* **375**, eabh3021 (2022).
34. A. Inutsuka *et al.*, The integrative role of orexin/hypocretin neurons in nociceptive perception and analgesic regulation. *Sci. Rep.* **6**, 29480 (2016).
35. K. Ghandour *et al.*, Orchestrated ensemble activities constitute a hippocampal memory engram. *Nat. Commun.* **10**, 2637 (2019).
36. S. Chowdhury *et al.*, Dissociating orexin-dependent and -independent functions of orexin neurons using novel Orexin-Flp knock-in mice. *Elife* **8**, e44927 (2019).
37. M. Mieda *et al.*, Orexin peptides prevent cataplexy and improve wakefulness in an orexin neuron-ablated model of narcolepsy in mice. *Proc. Natl. Acad. Sci. U.S.A.* **101**, 4649–4654 (2004).
38. A. Seifinejad, A. Vassalli, M. Tafti, Neurobiology of cataplexy. *Sleep Med. Rev.* **60**, 101546 (2021).
39. S. Zhou *et al.*, Activity of putative orexin neurons during cataplexy. *Mol. Brain.* **15**, 21 (2022).
40. T. E. Scammell, J. T. Willie, C. Guilleminault, J. M. Siegel, A consensus definition of cataplexy in mouse models of narcolepsy. *Sleep* **32**, 111–116 (2009).
41. A. Yamanaka *et al.*, Hypothalamic orexin neurons regulate arousal according to energy balance in mice. *Neuron* **38**, 701–713 (2003).
42. T. Tsunematsu *et al.*, Acute optogenetic silencing of orexin/hypocretin neurons induces slow-wave sleep in mice. *J. Neurosci.* **31**, 10529–10539 (2011).
43. T. Tsunematsu *et al.*, Long-lasting silencing of orexin/hypocretin neurons using archaerhodopsin induces slow-wave sleep in mice. *Behav. Brain Res.* **255**, 64–74 (2013).
44. R. H. Williams *et al.*, Transgenic archaerhodopsin-3 expression in hypocretin/orexin neurons engenders cellular dysfunction and features of type 2 narcolepsy. *J. Neurosci.* **39**, 9435–9452 (2019).
45. A. Vassalli *et al.*, Electroencephalogram paroxysmal theta characterizes cataplexy in mice and children. *Brain* **136**, 1592–1608 (2013).
46. S. Bastianini, A. Silvani, C. Berteotti, V. Lo Martire, G. Zoccoli, High-amplitude theta wave bursts during REM sleep and cataplexy in hypocretin-deficient narcoleptic mice. *J. Sleep Res.* **21**, 185–188 (2012).
47. K. F. Tanaka *et al.*, Expanding the repertoire of optogenetically targeted cells with an enhanced gene expression system. *Cell Rep.* **2**, 397–406 (2012).
48. S. Izawa *et al.*, REM sleep-active MCH neurons are involved in forgetting hippocampus-dependent memories. *Science* **365**, 1308–1313 (2019).
49. A. Yamanaka, Y. Muraki, N. Tsujino, K. Goto, T. Sakurai, Regulation of orexin neurons by the monoaminergic and cholinergic systems. *Biochem. Biophys. Res. Commun.* **303**, 120–129 (2003).
50. A. Yamanaka, S. Tabuchi, T. Tsunematsu, Y. Fukazawa, M. Tominaga, Orexin directly excites orexin neurons through orexin 2 receptor. *J. Neurosci.* **30**, 12642–12652 (2010).
51. T. Sakurai *et al.*, Input of orexin/hypocretin neurons revealed by a genetically encoded tracer in mice. *Neuron* **46**, 297–308 (2005).
52. C. B. Saper, P. M. Fuller, N. P. Pedersen, J. Lu, T. E. Scammell, Sleep state switching. *Neuron* **68**, 1023–1042 (2010).
53. J. Hara *et al.*, Genetic ablation of orexin neurons in mice results in narcolepsy, hypophagia, and obesity. *Neuron* **30**, 345–354 (2001).
54. S. Tabuchi *et al.*, Conditional ablation of orexin/hypocretin neurons: A new mouse model for the study of narcolepsy and orexin system function. *J. Neurosci.* **34**, 6495–6509 (2014).
55. F. Pizza *et al.*, Nocturnal sleep dynamics identify narcolepsy type 1. *Sleep* **38**, 1277–1284 (2015).
56. T. Nambu *et al.*, Distribution of orexin neurons in the adult rat brain. *Brain Res* **827**, 243–260 (1999).
57. J. John, M. F. Wu, L. N. Boehmer, J. M. Siegel, Cataplexy-active neurons in the hypothalamus: Implications for the role of histamine in sleep and waking behavior. *Neuron* **42**, 619–634 (2004).
58. L. Duffet *et al.*, A genetically encoded sensor for in vivo imaging of orexin neuropeptides. *Nat. Methods* **19**, 231–241 (2022).